Investigation of deuteron breakup and deuteron-induced fission on actinide nuclei at low incident energies

M. Avrigeanu* and V. Avrigeanu
Horia Hulubei National Institute for Physics and Nuclear Engineering, P.O. Box MG-6, 077125 Bucharest-Magurele, Romania

A. J. Koning
Nuclear Research and Consultancy Group, P.O. Box 25, NL-1755 ZG Petten, The Netherlands
(Received 9 December 2011; revised manuscript received 15 February 2012; published 12 March 2012)

The dominance of the deuteron breakup mechanism around the Coulomb barrier is shown by an analysis of the ^{231}Pa$(d, 3n)^{230}$U reaction excitation function, while the same attribute was found within a former assessment for the deuteron-induced fission. The present alternative result is obtained by taking into account, in addition to pre-equilibrium and compound-nucleus processes, the opposite effects of deuteron breakup, namely the decrease of the deuteron total reaction cross section, and the inelastic-breakup enhancement of various deuteron-induced reaction channels.

DOI: 10.1103/PhysRevC.85.034603 PACS number(s): 24.50.+g, 24.60.Dr, 25.45.Hi, 27.90.+b

I. INTRODUCTION

The analysis of deuteron-induced reactions at low energies, in terms of the usual nuclear reaction models, is challenging due to deuteron breakup as a result of its weak binding energy of 2.224 MeV. On the whole, the leakage of the initial deuteron flux toward the breakup process reduces the total reaction cross section that should be shared among different outgoing channels. On the other hand, a subsequent interaction between one of the deuteron constituents converted into breakup nucleons and the same target nucleus may lead through a secondary compound nucleus (CN) to enhancement of various reaction channels. In particular, the interaction with the target nucleus of a proton or neutron following a deuteron breakup is followed by cross-section enhancement for the (d, xn) and (d, xp) reactions, respectively.

These deuteron breakup (BU) effects are nicely illustrated in the case of the recently measured cross sections of the ^{231}Pa$(d, 3n)^{230}$U reaction between 11.2 and 19.9 MeV [1], which take advantage of quite recent ^{231}Pa$(p, 2n)^{230}$U reaction cross-section measurements [2] between 10.6 and 23.8 MeV. The particular value of the latter work comes from the superposition of its incident-energy range and the breakup proton energies corresponding to the energy range of Ref. [1], needed for accurate calculation of the BU enhancement of the $(d, 3n)$ reaction data. Thus we have found that the breakup is the main interaction process of deuterons with the ^{231}Pa target nucleus at the above-mentioned energies, while the same attribute was found previously [1] for deuteron-induced fission. First, this means that different ways may exist to describe the same data, so that additional measurements are needed in order to establish which description is better. Next, the proper handling of all breakup components should be pointed out for the ^{231}Pa$(d, 3n)^{230}$U reaction in the present work.

Conversely, later contributions to deuteron-induced reaction studies, e.g., [3] and references therein, have taken into account only the pre-equilibrium and fully equilibrated CN mechanisms, overlooking the deuteron breakup. As a result, either apparent discrepancies may occur between the calculated and experimental data or artificial changes of other model parameters could be triggered in order to get the data described by models. Nevertheless, a consistent analysis of deuteron interactions is of real interest for applied objectives such as fusion technology or nuclear medicine [1,3] as well as for basic issues related to, e.g., the surrogate nuclear reaction method ([4] and references therein). Thus one may note the rising use of the (d, xf) reaction, where x stands for a proton or deuteron, as a surrogate for the (n, f) reaction, and of $(d, p\gamma)$ as a surrogate for neutron capture. However, only the internal surrogate ratio method [5] was shown to be valid in the presence of the deuteron breakup without assuming a specific breakup mechanism.

Since the actual approach of the deuteron BU effects is discussed elsewhere [6–9], only basic formulas are reviewed in Sec. II along with notes on the competitive fission decay. The present detailed model calculation including the BU effects is given in Sec. III, emphasizing the role of the inelastic BU enhancement. Conclusions are given in Sec. IV. Preliminary results have been presented elsewhere [10].

II. DEUTERON BREAKUP AND INDUCED FISSION

A. Deuteron breakup cross sections

The physical picture of the deuteron breakup in the Coulomb and nuclear fields of the target nucleus considers two distinct processes, namely elastic breakup (EB), in which the target nucleus remains in its ground state and none of the deuteron constituents interacts with it, and inelastic breakup or breakup fusion (BF), where one of these deuteron constituents interacts with the target nucleus while the remaining one is detected (e.g., [8] and references therein). Under the assumption

*marilena.avrigeanu@nipne.ro

that the inelastic-breakup cross section for neutron emission, σ_{BF}^{n}, is the same as that for proton emission, σ_{BF}^{p}, the total breakup cross section σ_{BU} is given by the sum (e.g., Ref. [11]):

$$\sigma_{BU} = \sigma_{EB} + 2\sigma_{BF}^{n/p}, \quad (1)$$

while the total neutron- and proton-emission breakup cross sections, σ_{BU}^{n} and, respectively, σ_{BU}^{p}, are given by

$$\sigma_{BU}^{n/p} = \sigma_{EB} + \sigma_{BF}^{n/p}. \quad (2)$$

On the other hand, empirical parametrizations have been established [6] for the total nucleon-emission breakup fraction

$$f_{BU}^{(n/p)} = \sigma_{BU}^{n/p}/\sigma_{R} \quad (3)$$

and the elastic-breakup fraction

$$f_{EB} = \sigma_{EB}/\sigma_{R}, \quad (4)$$

where σ_R is the deuteron total reaction cross section. Since a dependence of these fractions on atomic Z and mass A numbers of the target nucleus and deuteron incident energy E was found on the basis of experimental systematics [6], the nucleon inelastic-breakup fraction may have the following form:

$$f_{BF}^{(n/p)} = f_{BU}^{(n/p)} - f_{EB}, \quad (5)$$

which leads to the nucleon inelastic-breakup cross sections

$$\sigma_{BF}^{n/p} = f_{BF}^{(n/p)}\sigma_{R}. \quad (6)$$

However, for $A \sim 230$ only the parametrization of the total nucleon-emission breakup fraction [6],

$$f_{BU}^{(n/p)} = 0.087 - 0.0066Z + 0.001\,63ZA^{1/3} + 0.0017A^{1/3}E - 0.000\,002ZE^{2}, \quad (7)$$

could be accurate, due to the lack of related data for the elastic breakup. In order to use the same approach for deuterons incident on the ^{231}Pa target nucleus and the energy range of the data of Ref. [1], we have taken into account the value $\sigma_{EB} = 119$ mb that was found [12] for deuterons incident on the ^{232}Th nucleus at $E = 15$ MeV as well as its normalization corresponding to the measured proton inelastic-breakup cross section within the same work. Moreover, due to the lack of additional similar data, we used the resulting value $f_{EB} = 0.164$ in the whole incident energy range, which is anyway rather narrow. Then we used the corresponding BU and BF components, given by Eqs. (5) and (7), to obtain the nucleon BF as well as the total BU cross sections shown in Fig. 1. In this respect, the deuteron total reaction cross section in Eqs. (3) and (6), respectively, is taken in the present work according to the RIPL-3 recommendation [13] for the deuteron optical potential of Ref. [14]. Actually, this potential is the only one based on the data analysis for nuclei with $A \geqslant 208$. The corresponding total reaction cross sections (Fig. 1) are larger than predictions of, e.g., the deuteron potential of Ref. [15], used within the computer code TALYS-1.2 [16]. They led to BU cross sections in the present work that are higher than the predictions of the Kalbach Walker parametrization [17] for the total neutron- and proton-emission breakup cross-sections and

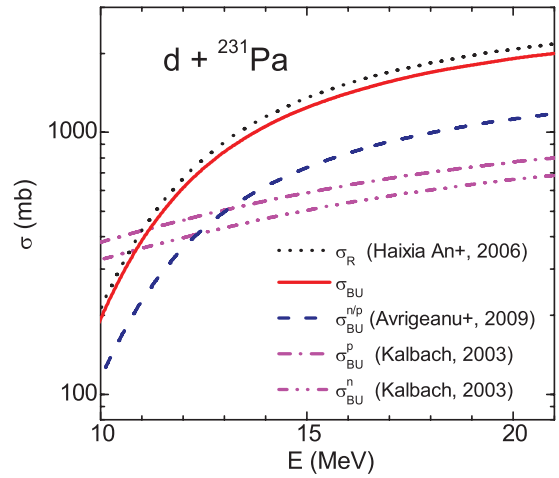

FIG. 1. (Color online) Energy dependence of the total breakup (solid curve), total nucleon-emission breakup cross sections (dashed curve) [6], and total proton–emission breakup cross section (dash-dotted curve) and neutron-emission breakup cross section (dash-dot-dotted) of Ref. [17], for deuterons interacting with ^{231}Pa around the Coulomb barrier. The deuteron total reaction cross sections [14] are also shown (dotted curve).

differ by normalization factors $K_{d,p/n}$:

$$\sigma_{BU}^{n/p} = K_{d,n/p}\frac{(A^{1/3}+0.8)^{2}}{1+\exp\frac{(13-E)}{6}}, \quad K_{d,n} = 18, \quad K_{d,p} = 21; \quad (8)$$

these are also shown in Fig. 1. Thus, for deuteron incident energies above ~13 MeV, the predictions for the total nucleon-emission breakup cross sections given by both parametrizations [6,17] are around ~50% of the deuteron total reaction cross section. It is only the extrapolation of the Kalbach Walker parametrization at low incident energies that leads to nucleon-emission BU cross sections exceeding even the deuteron total reaction cross section. Nevertheless, regardless of the differences between them, both parametrizations point out the dominance of the breakup mechanism at deuteron incident energies below and around the Culomb barrier. Actually, this conclusion is in line with the experimental total proton-emission BU fraction data for deuterons on ^{232}Th [12,18] that were taken into account within the above-mentioned systematics [6].

B. Fission competitive decay

On the other hand, Morgenstern *et al.* [1] have found a definite dominance of the fission decay channel within their former analysis of the ^{231}Pa$(d, 3n)^{230}$U reaction cross section around the Coulomb barrier. They also noted, although without a quantitative assessment, that a significant decrease of the available compound-nucleus cross section occurs due to the deuteron breakup. Nevertheless, the fission cross section obtained within the EMPIRE-2 computer code assumptions [19] has been quite close to the deuteron total reaction cross section (see Fig. 3 of Ref. [1]). Conversely, lower fission cross sections, explicitly shown in Fig. 2, can be found straight away using either the code TALYS [16] or the TENDL-2011

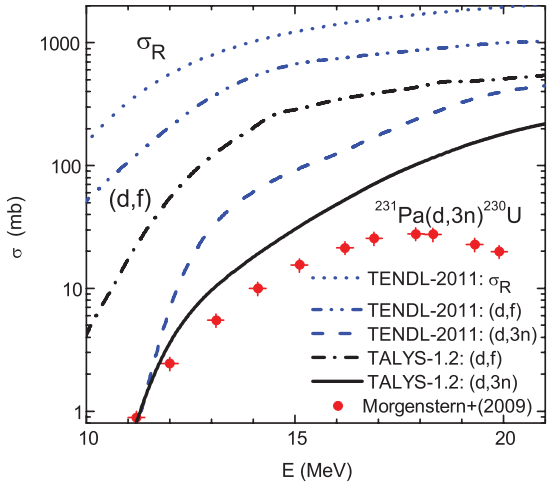

FIG. 2. (Color online) Comparison of the measured [1], calculated [16] (solid curve), and most recently evaluated [20] (dashed) excitation function of the reaction ^{231}Pa$(d, 3n)^{230}$U. Also shown are the corresponding calculated (dash-dotted curve) and evaluated (dash-dot-dotted) cross sections for the deuteron-induced fission on ^{231}Pa, together with the evaluated deuteron total reaction cross sections (dotted curve).

library [20]. The two distinct sets of calculated results are used here just to prove the similar weight of the fission mechanism. The significant difference between them is due to the different optical potentials used for deuterons, namely those of Watanabe [15] and Daehnick *et al.* [21], respectively. Unfortunately, there are no (d, f) measured cross sections but only an analysis of ^{231}Pa(d, pf) data at the deuteron energy of 15 MeV [22], where the measured fission probability versus the excitation energy of the residual nucleus ^{232}Pa was found to be lower than 40% (Fig. 16 from Ref. [22]). As a consequence, we focus on the measured ^{231}Pa$(d, 3n)^{230}$U excitation function in order to check the dominance of the breakup mechanism predicted by empirical parametrizations [6,17].

III. DETAILED BREAKUP MECHANISM

The dominance of the breakup mechanism has two opposite effects. First, the deuteron total breakup cross section reduces significantly the amount of total reaction cross section that should be shared among different outgoing channels. This effect is shown in Fig. 3(b) for the ^{231}Pa$(d, 3n)^{230}$U reaction and the calculated cross sections using the computer code TALYS-1.2 [16]. In order to emphasize the two distinct BU effects, we made a different choice than for the results shown in Fig. 2. Subsequently, we have not used the BU-inclusion option of TALYS by means of the Kalbach Walker parametrization [17]. Thus, we have obtained first the pre-equilibrium (PE) and CN contributions to the $(d, 3n)$ reaction cross sections, under the assumption of no breakup process. Then the BU reduction of these results was addressed by using a reduction factor $(1 - \sigma_{BU}/\sigma_R)$ of the deuteron total reaction cross section. The $(d, 3n)$ reaction cross sections obtained in this way are now in good agreement with the measured data just above the effective reaction threshold while formerly these data

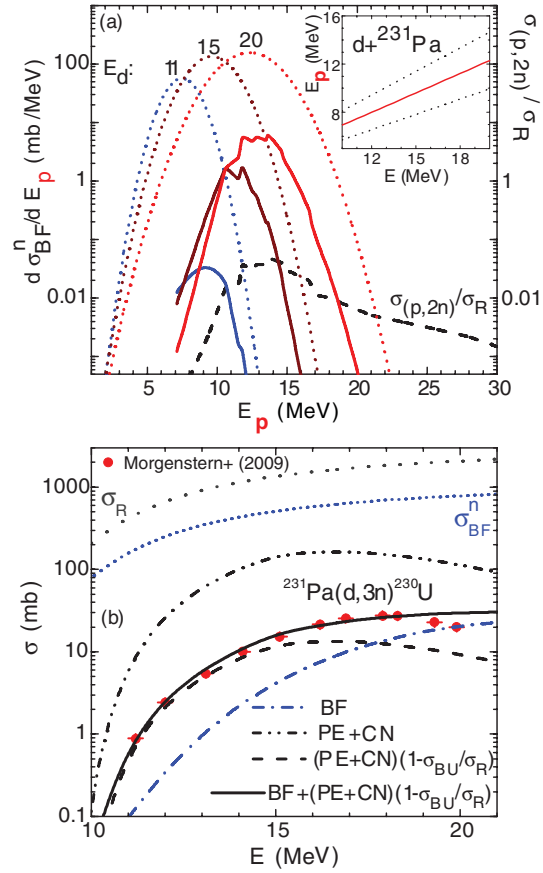

FIG. 3. (Color online) (a) Results (solid curves) of the convolution of the cross section ratio $\sigma_{(p,2n)}/\sigma_{(p,R)}$ for the target nucleus ^{231}Pa (dashed curve) with the Gaussian distribution (dotted curve) of breakup-proton energies for deuterons on ^{231}Pa at incident energies of 10, 15, and 20 MeV, as noted on their top; the insert shows the centroid of the Gaussian distribution of breakup-proton energies [26] vs the deuteron incident energy (solid curve) on ^{231}Pa and the related $E_p \pm \Gamma/2$ values (dashed curves). (b) The same as Fig. 2 but for deuteron total reaction cross section [14] (dotted curve), nucleon inelastic-breakup cross section (short dotted curve), BF enhancement (dash-dotted curve), and the $(d, 3n)$ reaction cross sections calculated without (dash-dot-dotted curve) and with (dashed curve) inclusion of the BU effect on σ_R, as well as of the BF enhancement (solid curve).

were also greatly overestimated. However, an underestimation by a factor up to 3 at $E \sim 20$ MeV becomes visible in Fig. 3(b). Nevertheless, the description of the reaction cross sections at the lowest energies may validate the PE and CN model parameters used in these calculations. Thereby, we used particularly the above-mentioned deuteron optical potential [14], the nucleon optical potentials for actinides [23] from the RIPL 2408 and RIPL 5408 potential segments [13] for neutrons and protons, respectively, the microscopic level densities of Goriely *et al.* [24], and the WKB approximation for the fission path model [25].

Second, we aim to account for the inelastic breakup (BF) enhancement due to one of the deuteron constituents that interacts with the target nucleus and leads to a secondary

CN, with further significant contributions to various deuteron-induced reaction channels. In the present case the absorbed proton, following the breakup neutron emission, contributes to the enhancement of the ^{230}U activation cross section through the ^{231}Pa$(p, 2n)^{230}$U reaction.

In order to calculate this breakup enhancement of the ^{231}Pa$(d, 3n)^{230}$U reaction, the nucleon BF cross section σ^n_{BF} given by Eq. (6) was formerly [10] multiplied by the ratio $\sigma_{(p,2n)}/\sigma_{(p,R)}$ that corresponds to the weight of the above-mentioned reaction induced by the breakup protons on the ^{231}Pa target nucleus [10]. We used in this respect the measured ^{231}Pa$(p, 2n)^{230}$U reaction cross sections [2] and the proton total reaction cross section $\sigma_{(p,R)}$ generated by the above-mentioned optical potential. We may express this ratio in terms of the deuteron incident energy, using the recent Kalbach Walker [26] formula for the center-of-mass system centroid of the Gaussian distribution of breakup-proton energies. Since the breakup-proton energy range of ∼9–14 MeV corresponds to incident energies of 11–20 MeV of the measured $(d, 3n)$ excitation function [2], the $\sigma_{(p,2n)}$ cross sections values are provided just by the measurements, with no other reaction model calculations being involved. This is why the simultaneous analysis of $(d, 3n)$ [1] and $(p, 2n)$ experimental excitation functions [2] is so useful for the study of the inelastic breakup and complementary reaction mechanisms considered for the deuteron interactions with nuclei.

However, a better estimation for the BF enhancement than the above multiplication of σ^n_{BF} by the ratio $\sigma_{(p,2n)}/\sigma_{(p,R)}$ in terms of deuteron energy is given by the convolution of the same ratio with the Gaussian distribution of the breakup-proton energies corresponding to a given incident deuteron energy [26]. The former as well as the latter quantities for three deuteron incident energies are shown in Fig. 3(a). The same method has previously been applied [9,10] using a former Gaussian line shape [17]. The areas of the related convolution results correspond to the BF enhancement of the $(d, 3n)$ reaction cross sections at the given deuteron energies. The energy dependence of this BF enhancement of the ^{231}Pa$(d, 3n)^{230}$U activation cross section is shown in Fig. 3(b), while the corresponding total activation of ^{230}U is finally compared with the experimental data [1]. As expected, the more realistic treatment of the BF enhancement by taking into account the quite large widths Γ of the breakup-proton energy distributions [see the upper insertion in Fig. 3(a)] has led to a rather accurate description of the data. Further improvements of the breakup analysis could add to a better account of the related energy dependence.

IV. CONCLUSIONS

The dominance of the deuteron breakup mechanism at energies around the Coulomb barrier is shown by an analysis of the ^{231}Pa$(d, 3n)^{230}$U reaction excitation function, while the same attribute was found within a former assessment [1] for the deuteron-induced fission. The present analysis has taken into account, in addition to the pre-equilibrium and compound-nucleus processes, the opposite effects of the deuteron breakup, namely the decrease of the deuteron total reaction cross section, and the BF enhancement of various deuteron-induced reaction channels.

The improvement of deuteron breakup effects estimation requires complementary experimental studies of, e.g., the $(d, 3n)$ and $(p, 2n)$ reaction cross sections for the same target nucleus and within correlated incident-energy ranges. The suitability of the empirical parametrization of the breakup components and reaction mechanisms involved in the interaction process could thus be checked and updated. Furthermore, associated inclusive neutron and proton spectra measurements that allow the distinction among various contributing mechanisms are greatly needed too, as well as (d, pf) angular correlations when the deuteron-induced fission process is analyzed. Given the increased interest in surrogate reaction studies, e.g., Ref. [27], the usefulness of detailed theoretical and experimental investigations of the breakup of weakly bound projectiles including deuterons is obvious.

ACKNOWLEDGMENTS

This work was partly supported by a grant from the Romanian National Authority for Scientific Research, CNCS-UEFISCDI, project No. PN-II-ID-PCE-2011-3-0450.

[1] A. Morgenstern, O. Lebeda, J. Stursa, R. Capote, M. Sin, F. Bruchertseifer, B. Zielinska, and C. Apostolidis, Phys. Rev. C **80**, 054612 (2009).
[2] A. Morgenstern, O. Lebeda, J. Stursa, F. Bruchertseifer, R. Capote, J. McGinley, G. Rasmussen, M. Sin, B. Zielinska, and C. Apostolidis, Anal. Chem. **80**, 8763 (2008) [www-nds.iaea.or.at/exfor]; A. Morgenstern *et al.*, EXFOR D0562 entry.
[3] A. Hermanne, R. Adam Rebeles, F. Tarkanyi, S. Takacs, M. P. Takacs, J. Csikai, and A. Ignatyuk, Nucl. Instrum. Methods, Sec. B **270**, 105 (2012); F. Ditroi, F. Tárkányi, S. Takács, A. Hermanne, A. V. Ignatyuk, and M. Baba, *ibid.* **270**, 61 (2012).
[4] S. Chiba and O. Iwamoto, Phys. Rev. C **81**, 044604 (2010).
[5] J. M. Allmond *et al.*, Phys. Rev. C **79**, 054610 (2009).
[6] M. Avrigeanu, W. von Oertzen, R. A. Forrest, A. C. Obreja, F. L. Roman, and V. Avrigeanu, Fusion Eng. Des., **84**, 418 (2009).
[7] P. Bém, E. Šimečková, M. Honusek, U. Fischer, S. P. Simakov, R. A. Forrest, M. Avrigeanu, A. C. Obreja, F. L. Roman, and V. Avrigeanu, Phys. Rev. C **79**, 044610 (2009).
[8] M. Avrigeanu and A. M. Moro, Phys. Rev. C **82**, 037601 (2010).
[9] E. Šimečková, P. Bém, M. Honusek, M. Štefánik, U. Fischer, S. P. Simakov, R. A. Forrest, A. J. Koning, J.-C. Sublet, M. Avrigeanu, F. L. Roman, and V. Avrigeanu, Phys. Rev. C **84**, 014605 (2011).
[10] M. Avrigeanu, V. Avrigeanu, and F. L. Roman, EPJ Web Conf. **21**, 07003 (2012).
[11] M. G. Mustafa, T. Tamura, and T. Udagawa, Phys. Rev. C **35**, 2077 (1987).

[12] J. Kleinfeller, J. Bisplinghoff, J. Ernst, T. Mayer-Kuckuk, G. Baur, B. Hoffmann, R. Shyam, F. Rosel, and D. Trautmann, Nucl. Phys. A **370**, 205 (1981).
[13] R. Capote *et al.*, Nucl. Data Sheets **110**, 3107 (2009) [http://www-nds.iaea.org/RIPL-3/].
[14] H. An and C. Cai, Phys. Rev. C **73**, 054605 (2006).
[15] S. Watanabe, Nucl. Phys. **8**, 484 (1958).
[16] A. J. Koning, S. Hilaire, and M. C. Duijvestijn, TALYS-1.0, in *Proceedings of the International Conference on Nuclear Data for Science and Technology, Nice, 2007*, edited by O. Bersillon, F. Gunsing, E. Bauge, R. Jacqmin, and S. Leray (EDP Sciences, Paris, 2008), p. 211; version TALYS-1.2, December 2009 [http://www.talys.eu/home/].
[17] C. Kalbach Walker, TUNL Progress Report XLII (2002-2003), Triangle University Nuclear Laboratory, 2003, pp. 82-83 [www.tunl.duke.edu/publications/tunlprogress/2003/].
[18] J. R. Wu, C. C. Chang, and H. D. Holmgren, Phys. Rev. C **19**, 370 (1979).
[19] M. Herman, R. Capote, B. V. Carlson, P. Oblozinsky, M. Sin, A. Trkov, H. Wiencke, and V. Zerkin, Nucl. Data Sheets **108**, 2655 (2007).
[20] A. J. Koning and D. Rochman, TENDL-2011: TALYS-Based Evaluated Nuclear Data Library (November 21, 2011) [http://www.talys.eu/tendl-2011/].
[21] W. W. Daehnick, J. D. Childs, and Z. Vrcelj, Phys. Rev. C **21**, 2253 (1980).
[22] B. B. Back, H. C. Britt, O. Hansen, B. Leroux, and J. D. Garrett, Phys. Rev. C **10**, 1948 (1974).
[23] R. Capote, S. Chiba, E. Soukhovitskii, J. M. Quesada, and E. Bauge, J. Nucl. Sci. Technol. **45**, 333 (2008).
[24] S. Goriely, S. Hilaire, and A. J. Koning, Phys. Rev. C **78**, 064307 (2008).
[25] M. Sin, R. Capote, and A. Ventura, M. Herman, and P. Obložinský, Phys. Rev. C **74**, 014608 (2006).
[26] C. Kalbach Walker, 1st Research Co-ordination Meeting of the Fusion Evaluated Nuclear Data Library FENDL 3.0, 2–5 December 2008, IAEA, Vienna [http://www-nds.iaea.org/fendl3/RCM1_documents.html].
[27] B. Jurado *et al.*, Workshop on Nuclear Data Measurements, Nov. 28-29, 2011, Issy-les-Moulineaux [http://www.gedeon.prd.fr/].